

# Conjunction Risk Assessment and Avoidance Maneuver Planning Tools

Saika Aida

*DLR German Space Operations Center (GSOC), Oberpfaffenhofen, 82234 Weßling, Germany  
+49 8153 28-2158, [saika.aida@dlr.de](mailto:saika.aida@dlr.de)*

## ABSTRACT

In the collision avoidance operation, earlier estimation of possible critical conjunctions among other events is important to handle critical situations promptly and efficiently. Additionally, earlier estimation of the possible avoidance maneuver strategy is also important due to the limited time until the closest approach. The presented tools for the collision risk assessment and the avoidance maneuver planning are based on the collision probability and the relative position visualization in the B-plane. Visualization of the object trajectory due to the orbit uncertainty and also due to the avoidance maneuver facilitates an estimation of the possible risk and the maneuver effect. Application of the tools to the operational collision avoidance process is also presented, together with the conjunction handling of two operational satellites flying in a very close formation, where the tools are especially useful to handle the complicated operational requirements.

**Index Terms**— Collision risk, Avoidance maneuver, Collision probability, B-plane

## 1. INTRODUCTION

The ever increasing number of objects in the near Earth region has been causing growing concerns about the space environment and accordingly about the safety of future space missions. Since most of orbital debris stay in the orbit for years, even a single collision between space objects could seriously increase the debris population, making further collisions more likely.

The German Space Operations Center (GSOC) has been performing collision avoidance operation since 2009. Additional to the operational satellites currently 5 in LEO and 2 in GEO, conjunction monitoring and mitigation for several satellites are supported, which are operated by other organizations or ended the operation phase. The Conjunction Data Message (CDM) provided by the Joint Space Operations Center (JSpOC) is currently the main source for the orbital information of the space objects due to the quality and timeliness of the available information. Conjunction prediction, risk assessment, and avoidance

maneuver analysis are performed automatically in the operational process.

In the collision avoidance operation, numerous conjunctions are reported daily, which were detected within certain thresholds. Earlier estimation of possible critical conjunctions among all predicted events is therefore important to handle critical situations promptly and efficiently. Additionally, earlier estimation of the possible avoidance maneuver strategy is also important, because a decision of the avoidance maneuver execution is mostly done within one day before the closest approach based on the latest prediction. Especially, two operational satellites TerraSAR-X and TanDEM-X are flying in a very close formation with a minimum distance of ~300 m, therefore the avoidance maneuver for both satellites shall be taken into account to handle close approaches of each encountering object. The avoidance strategies to meet the control requirements and to optimize the maneuver shall be investigated in the limited time.

In the paper, algorithms for the conjunction risk assessment and the avoidance maneuver analysis are described, followed by a presentation of their application in the automated collision avoidance process to facilitate handling of critical conjunctions. The past conjunction example and the lessons are also presented.

## 2. CONJUNCTION RISK ASSESSMENT

The detected conjunctions are analyzed using several risk assessment tools. One of the tools is introduced in this section, which visualizes the collision probability and the conjunction geometry for the short-term encounter.

### 2.1. Collision Probability Calculation

Several methods for the collision probability calculation for the short-term encounter have been developed. In the applied method, the collision probability is calculated based on the hitradius, the orbital states, and covariance information at the time of the closest approach (TCA). The hitradius is defined as a sum of each object radius and the shape is considered as a sphere, so that the object attitude at the conjunction is not taken into account. The position uncertainty is described by a 3D Gaussian distribution, and

the velocity uncertainty is neglected. The position uncertainty of two objects is assumed to be uncorrelated. For the short-term encounter, two objects are assumed to be moving along straight lines at constant velocities, and the position uncertainty during the encounter is also assumed to be constant. Using these assumptions, the collision probability mapped onto the B-plane is expressed as Eq. 1 [1]. The B-plane is perpendicular to the relative velocity vector at TCA.

$$P_c = \frac{1}{2\pi \cdot \sqrt{\det(C_B)}} \cdot \int_{-R_c}^{R_c} \int_{-\sqrt{R_c^2-x^2}}^{\sqrt{R_c^2-x^2}} \exp\left[-\frac{1}{2} \Delta \hat{r}_B^T C_B^{-1} \Delta \hat{r}_B\right] dy dx \quad (1)$$

$R_c$  is the hitradius centered at the predicted fly-by location.  $\Delta \hat{r}_B$  and  $C_B$  represent the projected position vector and covariance matrix. The maximum collision probability can be also calculated by scaling the covariance matrix by a factor  $k^2$  [2]:

$$P_{c,max} = \frac{R_c^2}{\exp(1) \sqrt{\det(C_B)} \cdot \Delta \hat{r}_B^T C_B^{-1} \Delta \hat{r}_B} \quad (2)$$

$$k^2_{p,max} = \frac{1}{2} \Delta \hat{r}_B^T C_B^{-1} \Delta \hat{r}_B \quad (3)$$

For a very small covariance ellipse, the relative position is far away from the ellipse center, which results in the small collision probability. As the covariance ellipse size increases, the probability reaches a maximum. Further increment of the covariance ellipse size leads to a dilution in the probability computation [3]. In such cases the maximum probability in Eq. 2 is applied instead of the unscaled one in Eq. 1 so that the collision probability is not underestimated due to the large orbit uncertainties.

## 2.2. Collision Probability Expressed by Covariance Scaling Factor

When the B-plane axes are aligned with the minor/major axes of the projected covariance ellipse and the probability is assumed to be constant within the integration radius, with its value taken at the integration center, Eq. 1 and Eq. 2 can be written in the following forms:

$$P_c = \frac{R_c^2}{2 \cdot \sigma_x \sigma_y} \cdot \exp\left[\left(-\frac{1}{2}\right) \cdot l^2\right] \quad (4)$$

$$P_{c,max} = \frac{R_c^2}{\exp(1) \cdot \sigma_x \sigma_y} \cdot \frac{1}{l^2} \quad (5)$$

$$l^2 = \left\{ \left( \frac{x_m}{\sigma_x} \right)^2 + \left( \frac{y_m}{\sigma_y} \right)^2 \right\} \quad (6)$$

$x_m$  and  $y_m$  are the respective components of the projected miss distance, and  $\sigma_x$  and  $\sigma_y$  are the corresponding standard deviations. Note that Eq. 6 indicates that the projected relative position lies along the scaled covariance ellipse with a factor of  $l$ .

## 2.3. Probability Accuracy Evaluation

Eq. 4 and Eq. 5 were derived on the assumption that the probability is constant within the integration radius. The accuracy of the approximate probability in Eq. 4 was evaluated by a comparison with numerical results.

The probability along the covariance ellipse minor axis was calculated for different ellipse size with the fixed ratio (AR=10) of the major axis to the minor axis. In Figure 1, two plots are shown for different hitradius. For each plot, the x-axis shows the ratio of the position (X) to the corresponding minor axis (sigX). For a larger ellipse size, the approximate values match well with the numerical results. However, when the hitradius is large (~10 m) and the ellipse size is small (~10 m), the error is not negligible especially for lower probabilities.

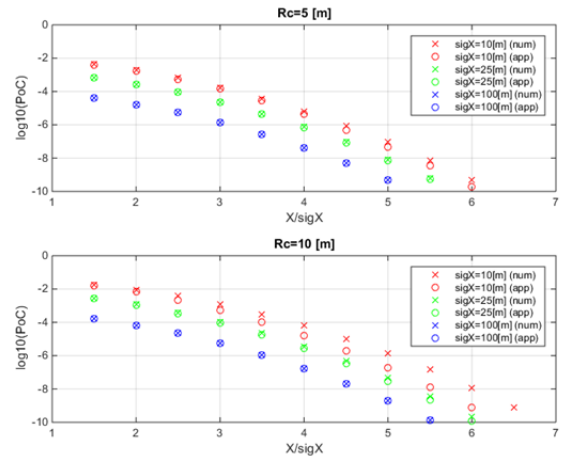


Figure 1 Probability Comparison with Numerical Results (AR=10)

## 2.4. Collision Probability and Geometry Visualization in B-plane

Using Eq. 4 - Eq. 6, the collision probability contour lines can be plotted in the B-plane, which are along with the scaled covariance ellipse projected onto the B-plane. An

example of the operational satellite TerraSAR-X conjunction with the COSMOS 405 satellite is shown in Figure 2. The primary object (TerraSAR-X) position is set as the center, and the secondary (COSMOS 405) position relative to the primary is plotted with a circle. The X-axis of the B-plane is chosen so that it nearly corresponds to the radial direction of the primary object. Additionally, the distance from the center corresponds to the relative distance.

In Figure 2, the collision probability at different positions is shown by the contour lines in different colors. The maximum collision probability in Eq. 5 becomes equal to the unscaled one in Eq. 4, when the covariance scaling factor is  $l^2=2$ . Inside this area ( $l^2<2$ ), the maximum collision probability is applied. This area is also distinguished by the different color.

In low earth orbits, the largest orbit uncertainty is in the along-track direction due to the atmospheric influence [4], which causes variations of the conjunction geometry as well as the TCA in different predictions. In the current operational process, the prediction is updated several times per day based on the latest orbit information, starting from TCA-7.0 days for LEO satellites, and TCA-14.0 days for GEO satellites. Considering the along-track error for both of the primary and secondary objects, the path of the relative position in the B-plane is additionally plotted in Figure 2. The bold line is the path based on the  $3\sigma$  positional uncertainties in the along-track direction, showing that the relative position can vary close to the corresponding line in the upcoming predictions. Note that the B-plane at different TCAs does not exactly match the original one. However, the variation of the TCA in the consecutive predictions is small, e.g. several hundred milliseconds, therefore the original B-plane is still applicable to the path plot.

### 3. AVOIDANCE MANEUVER PLANNING

When a possible critical conjunction is detected, the avoidance maneuver analysis is automatically performed so that the operator can assess possible maneuver options, taking into account the orbit control requirements of the satellite and the timeline. The avoidance maneuver analysis tool for a single object encounter is introduced in this section.

#### 3.1. Avoidance Maneuver Analysis

The conjunction risk assessment tool described in section 2 is applied to the avoidance maneuver analysis tool. The purpose of the tool is to visualize the effect of several maneuver options, which are different in size, direction, and epoch, to the collision probability as well as the conjunction geometry. Based on the results, the operator selects a suitable solution which reduces the collision risk and also meets the operational requirements.

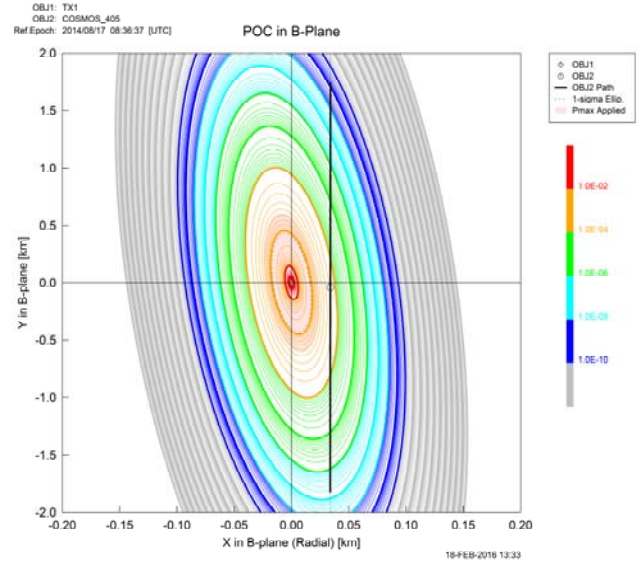


Figure 2 Collision Probability and Geometry Visualization

#### 3.2. Thrusting Selection and Implementation

For avoidance maneuver simulation, only in-track thrusting is taken into account. Compared to general thrusting, in-track thrusting is much simpler to implement and also much simpler to execute operationally for spacecraft maneuvers. In fuel expenditure, it is only slightly more costly than the more general approach in the case of only one collision avoidance maneuver [5]. Additionally, in-track thrusting is effective in the long run, if there is a complementary adjustment to bring the spacecraft back to the original orbit.

In-track thrusting causes tangential shifts, which is estimated by the following equation:

$$\Delta D_T \approx 3 \cdot \Delta v \cdot \Delta t \quad (7)$$

where  $\Delta D_T$  is the relative distance increment in tangential direction,  $\Delta v$  is the velocity increment in tangential direction, and  $\Delta t$  is the time between TCA and the maneuver epoch. The corresponding change in the semi-major axis  $a$  can be computed by

$$\Delta a \approx 2 \cdot \frac{\Delta v}{v} \cdot a \quad (8)$$

To increase the radial distance, a tangential maneuver has to be placed at an argument of latitude  $180^\circ$  off from the argument of latitude at the close approach. In this case, the radial distance increment  $\Delta D_R$  at the close approach is estimated as follows:

$$\Delta a = \frac{\Delta D_R}{2} \approx 2 \cdot \frac{\Delta v}{v} \cdot a \quad (9)$$

In the maneuver simulation, the propagation is done by assuming a pure Kepler orbit to reduce the computation time. The initial state vector of the primary object at the original TCA is propagated backwards to the maneuver epoch. The velocity change is then applied to the state vector along the appropriate axis, and propagated forwards to the original TCA. Using the new state vector for the primary object, the conjunction near the original TCA is calculated by the linear interpolation. The covariance near the TCA is assumed static and therefore not propagated.

### 3.3. Maneuver Effect Visualization in B-plane

The maneuver analysis plot is shown in Figure 3, using the same example of the conjunction between TerraSAR-X and COSMOS 405 as used in Figure 2. For maneuver options, four in-track maneuvers are configured as default, which are different in size and direction (flight direction or reverse). In the operational process, the maneuver size of 1.0 cm/s and 2.0 cm/s are implemented for the operational LEO satellites (altitude range between 400 km and 510 km). The maneuver size required to achieve the safety criteria was evaluated based on the standard deviations for the past conjunctions [6].

For each maneuver option, the trajectory of the resulting relative position at the closest approach due to the corresponding maneuver at the different epoch (starting from TCA-0.0 hour) is plotted in different colors and line styles. In Figure 3, the earliest maneuver epoch is set to TCA-6.0 hours. For each trajectory, the maximum radial separation is achieved by maneuvers performed at TCA-(odd)×(half orbital period) according to Eq. 9. The relative position shifts along the path line shown in Figure 2 for maneuvers at TCA-(even)×(half orbital period), which is due to the tangential shifts of the maneuvered object according to Eq. 7. The collision probability and the relative distance in radial (R), along-track (T), and out-of plane (N) depending on the different maneuver epoch are shown in Figure 4.

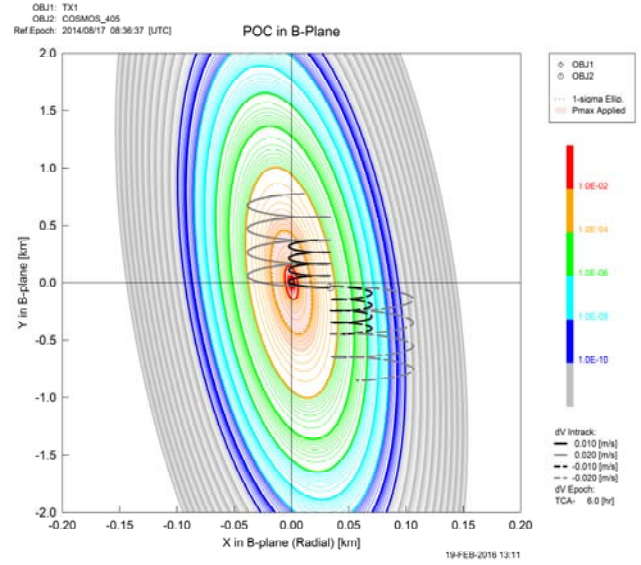


Figure 3 Maneuver Effect Visualization

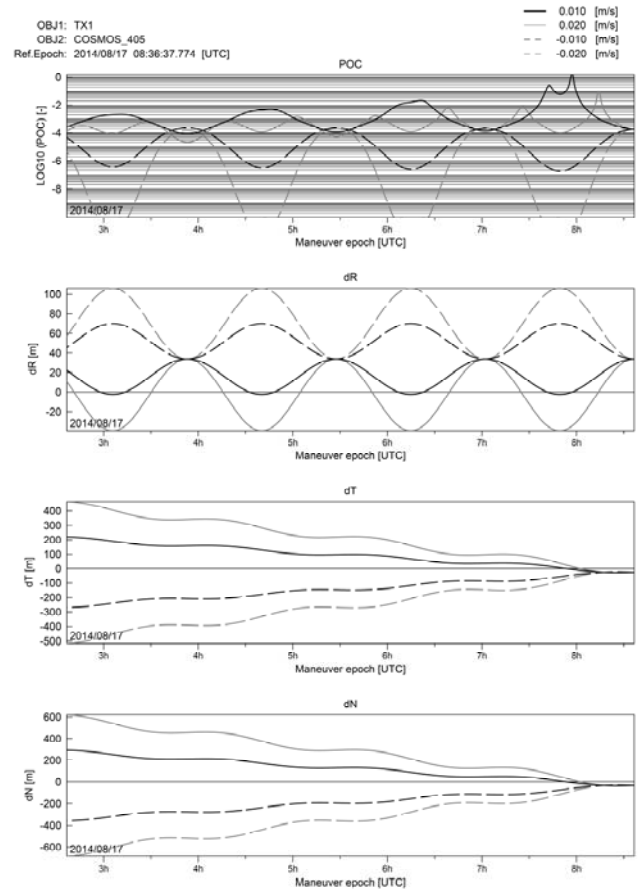


Figure 4 PoC and Relative Distance for Different Maneuver Epoch

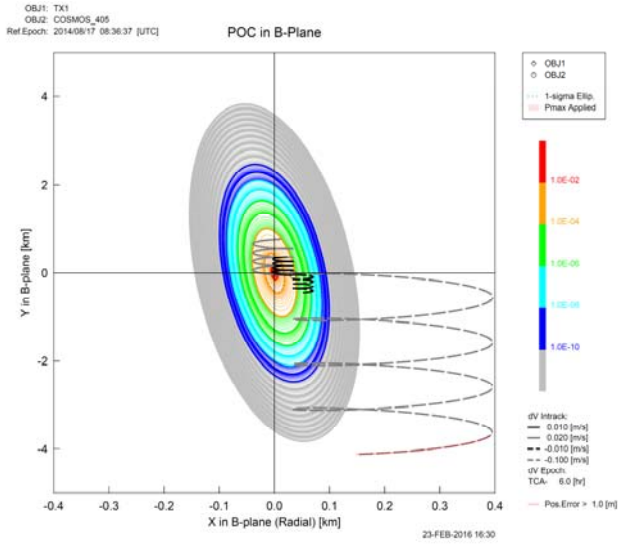


Figure 5 Maneuver Effect Visualization

### 3.4. B-plane Error Evaluation

When an avoidance maneuver is performed, the conjunction geometry as well as the timing of the closest approach changes accordingly. Therefore the B-plane for each predicted conjunction differs slightly from the original one which is defined for the initial TCA. The difference cannot be negligible when the maneuver size is large, or the maneuver timing is much prior to the TCA, which leads to the large positional error and accordingly the collision probability error in the B-plane plot. To evaluate the error, the trajectory is distinguished when the relative position for the corresponding B-plane differs from the one for the original plane more than the pre-defined tolerance.

In Figure 5, the positional error tolerance is set to 1.0 m for the same conjunction shown in Figure 3. The trajectory which violates the tolerance is plotted in the different color. It can be recognized when the maneuver size is -10.0 cm/s and the maneuver epoch is more than ~3.5 orbits prior to the TCA. However, the maneuver size is higher than the estimated value of a few cm/s, and the maneuver epoch is also earlier than the nominal maneuver timing of 0.5-1.5 orbits before TCA. Therefore, the positional error in the B-plane plot due to the avoidance maneuver is negligible for the nominal case.

## 4. APPLICATION TO OPERATIONAL PROCESS

### 4.1. Operational Collision Avoidance

The collision avoidance process consists of mainly three steps: conjunction detection, risk analysis and mitigation.

The main source for the conjunction detection is the CDM provided by JSpOC. When a CDM is reported to the GSOC Flight Dynamics, the message is processed and the screening is performed using the satellite orbit data. For each conjunction, the prediction list and additionally the conjunction analysis results are generated and delivered per E-mail to the corresponding project members. The conjunction analysis results include the geometry plot, the probability B-plane plot as described in section 2, and the prediction history plot. When a possible critical conjunction is detected ( $PoC > 1.0 \times 10^{-5}$ ), additional products are generated, which include the maneuver analysis plot introduced in section 3, and also ground contact opportunities for additional radar tracking, which is planned to improve the orbit accuracy of the encountering object if necessary. The whole process mentioned above is running automatically. Based on the delivered products, the flight dynamics engineer decides further actions (ignore, mitigate, or perform radar tracking).

### 4.2. TerraSAR-X and TanDEM-X Conjunction Handling

Two operational satellites TerraSAR-X (TSX) and TanDEM-X (TDX) are flying in a very close formation with a minimum distance of ~300 m, therefore the avoidance maneuver for both satellites shall be taken into account to handle close approaches of each encountering object. Due to the high orbit control requirements of these satellites [7], the following precautions exist in principle in case of a significant risk. If the risk applies only to TSX, there are three collision avoidance scenarios:

- A. Change execution time and size of a regular TSX maneuver, TDX replicates the maneuver, or
- B. TSX performs two maneuvers for collision avoidance and re-acquisition of reference orbit, and
  - B1. TDX replicates the maneuvers (fuel-expensive), or
  - B2. TDX remains passive and the formation has to be re-acquired by TDX afterwards (time-consuming).

If only TDX is affected, TSX remains passive and TDX has to perform maneuvers for collision avoidance and formation re-acquisition.

In the operational process, the updated prediction and other products are generated for both satellites when one of these satellites receives a CDM. In case of a critical conjunction, the maneuver analysis is also performed for both satellites and the appropriate maneuver option is discussed which meets the control requirements and optimizes the maneuver. A past example is shown in Figure 6 for TX1 and Figure 7 for TDX for the same encountering object on 2014/08/17. The figures show that the critical conjunction ( $PoC > 1.0 \times 10^{-4}$ ) is only for TSX, and an in-

track maneuver of 1.0 cm/s in the anti-flight direction reduces the collision probability to lower than  $1.0 \times 10^{-6}$ . On the other hand, the TDX conjunction is not critical ( $PoC < 1.0 \times 10^{-10}$ ), and the replication of the avoidance maneuver does not lead to the critical conjunction. As a result, an avoidance maneuver of -0.5 cm/s a half orbit before the TCA was selected for both satellites, which satisfied the satellite control requirements. Therefore, no correction maneuver was necessary after TCA.

## 5. CONCLUSION

Tools for the conjunction risk assessment and the avoidance maneuver planning for the short-term single encounter were presented. Both tools are based on the collision probability and the relative position visualization in the B-plane. Application of the tools to the operational collision avoidance process was also presented, together with the conjunction handling of two satellites flying in a very close formation, where the tools are especially useful to handle the complicated operational requirements.

## 6. REFERENCES

- [1] Foster, J. and Estes, H. "A Parametric Analysis of Orbital Debris Collision Probability and Maneuver Rate for Space Vehicles." NASA/JSC-25898 August 1992.
- [2] Alfriend, K., Akella, M., Lee, D., Frisbee, J., Foster, J., Lee, D., and Wilkins, M. "Probability of Collision Error Analysis." Space Debris Vol. 1 No. 1 (1999) pp. 21-35 Springer.
- [3] Alfano, S. "Relating Position Uncertainty to Maximum Conjunction Probability." AAS/AIAA Paper 03-548.
- [4] Aida, S. and Kirschner, M. "Collision Risk Assessment and Operational Experiences for LEO Satellites at GSOC." 22nd International Symposium on Spaceflight Dynamics, Sao Jose dos Campos, Brazil. Feb. 28 - Mar. 4, 2011.
- [5] F. Kenneth Chan. "Spacecraft Collision Probability." Chapter.7
- [6] Aida, S. and Kirschner, M. "Critical Conjunction Detection and Mitigation." 25th International Symposium on Spaceflight Dynamics, Munich, Germany. Oct. 19-23, 2015.
- [7] Kahle, R., Wermuth, M., Schlepp, B., and Aida, S. "The TerraSAR-X/TanDEM-X Formation Flight: Challenges to Flight Dynamics and First Results." 4th International Conference on Spacecraft Formation Flying Missions & Technologies, St-Hubert, Quebec. May 18-20, 2011.

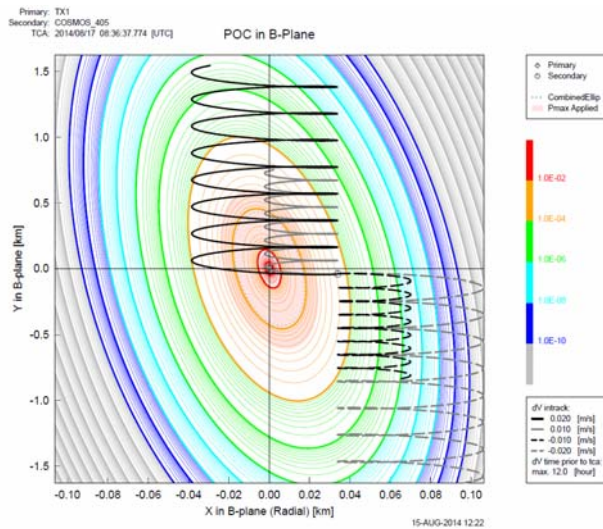


Figure 6 Maneuver Plot for Past Conjunction (TSX)

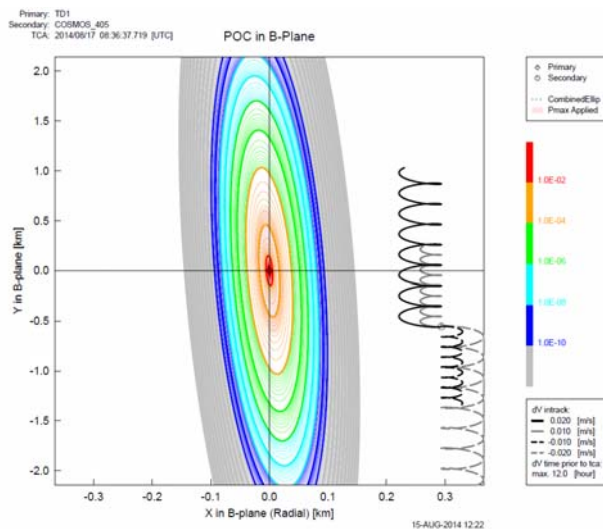


Figure 7 Maneuver Plot for Past Conjunction (TDX)